Defining a model of 3D seismogenic sources for Seismic Hazard Assessment applications: The case of central Apennines (Italy)

Article *in* Journal of Seismology · July 2004

DOI: 10.1023/B:JOSE.0000038449.78801.05

3 authors:

Paolo Boncio
Università degli Studi G. d'Annunzio Chieti …
79 PUBLICATIONS **1,338** CITATIONS
SEE PROFILE

Giusy Lavecchia
Università degli Studi G. d'Annunzio Chieti …
138 PUBLICATIONS **2,385** CITATIONS
SEE PROFILE

B. Pace
Università degli Studi G. d'Annunzio Chieti …
57 PUBLICATIONS **537** CITATIONS
SEE PROFILE

Journal of Seismology **8:** 407–425, 2004.

Defining a model of 3D seismogenic sources for Seismic Hazard Assessment applications: The case of central Apennines (Italy)

Paolo Boncio*, Giusy Lavecchia & Bruno Pace
Geodynamics and Seismogenesis Laboratory, Dipartimento di Scienze della Terra, Università "G. d'Annunzio" – Campus Universitario, 66013 Chieti, Italy
**author for correspondence: e-mail: pboncio@unich.it*

Received 14 March 2003; accepted in revised form 13 January 2004

Key words: active fault, earthquake, maximum expected magnitude, rheology, seismic hazard, seismogenic source, segmentation, structural geology

Abstract

Geology-based methods for Probabilistic Seismic Hazard Assessment (PSHA) have been developing in Italy. These methods require information on the geometric, kinematic and energetic parameters of the major seismogenic faults. In this paper, we define a model of 3D seismogenic sources in the central Apennines of Italy. Our approach is mainly structural-seismotectonic: we integrate surface geology data (trace of active faults, i.e. 2D features) with seismicity and subsurface geological–geophysical data (3D approach). A fundamental step is to fix constraints on the thickness of the seismogenic layer and deep geometry of faults: we use constraints from the depth distribution of aftershock zones and background seismicity; we also use information on the structural style of the extensional deformation at crustal scale (mainly from seismic reflection data), as well as on the strength and behaviour (brittle versus plastic) of the crust by rheological profiling. Geological observations allow us to define a segmentation model consisting of major fault structures separated by first-order (kilometric scale) structural-geometric complexities considered as likely barriers to the propagation of major earthquake ruptures. Once defined the 3D fault features and the segmentation model, the step onward is the computation of the maximum magnitude of the expected earthquake (M_{max}). We compare three different estimates of M_{max}: (1) from association of past earthquakes to faults; (2) from 3D fault geometry and (3) from geometrical estimate 'corrected' by earthquake scaling laws. By integrating all the data, we define a model of seismogenic sources (seismogenic boxes), which can be directly used for regional-scale PSHA. Preliminary applications of PSHA indicate that the 3D approach may allow to hazard scenarios more realistic than those previously proposed.

Introduction

Italy has a long history of large and moderate earthquakes, with an impressive amount of written information, which has been routinely used for statistical hazard analyses. The Italian catalogue reports information on earthquakes dating back to 461 BC, but it may be considered complete only for 400 to 1000 years, depending on the felt area and the intensity of the earthquake (see the discussion in Peruzza, 1999). Geological and paleoseismological investigations show that large earthquakes may have long recurrence intervals (of the order of 1000 years or more; Barchi et al., 2000; Valensise and Pantosti, 2001 and references therein). These considerations contradict the assumption, implicit in the historical probabilistic seismic hazard methods, that the historical record is representative of the activity of all the seismogenic sources (see Sleiko et al., 1998 for application of these methods to Italy). For these reasons, new models and methods for probabilistic seismic hazard assessment (PSHA) have been developing in Italy. These methods require the transition from catalogue-based probabilistic seismic hazard estimates to geology-based time-dependent PSHA (e.g. Peruzza, 1999). The new PSHA methodologies require information on the geometric, kinematic and

energetic parameters of the major seismogenic faults, so that constrains based on independent geological evidence could be introduced on the characterisation of the seismicity.

Recent applications of geology-based PSHA to central Italy (Peruzza, 1999; see Figure 1a for a possible scenario) have been performed, by considering the surface trace of active faults as input parameters. Using surface data alone (faults by geological mapping) may create some problems in assessing the seismic hazard. Surface data allow to define 2D linear features. Linear features may allow, under a number of assumptions, to estimate the maximum expected magnitude, by using empirical relationships (e.g. Wells and Coppersmith, 1994). Nevertheless, when they are used as input parameters for PSHA, they become the sources which radiate the seismic energy. Obviously, linear faults are far from representing both the real radiating-energy sources and the likely epicentres of the associated expected earthquakes. The real seismogenic sources are fault surfaces, the shape and area of which can be completely defined only by knowing the fault geometry at depth: inclination and listric versus planar geometry of the fault plane, thickness of the seismogenic layer (i.e. the down-dip extent of the seismogenic fault plane) and segmentation pattern. Therefore, the consideration of the third dimension is essential for a more realistic definition of seismogenic sources.

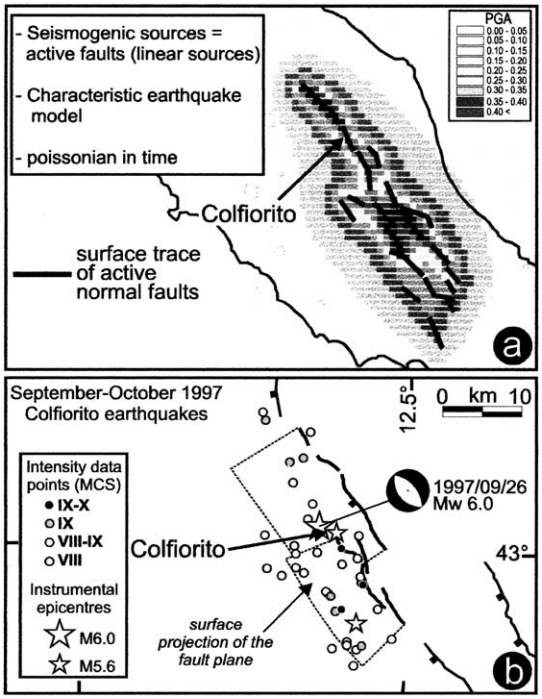

Figure 1. (a) Example of possible seismic hazard scenario for the central Apennines of Italy (from Peruzza, 1999) obtained by using 2D seismogenic sources (surface trace of active faults); (b) macroseismic field of the 1997 Colfiorito earthquakes (intensity data points larger than VII–VIII on the MCS scale) illustrating the relative position of the maximum damage compared to the geometry of the normal faults activated during the seismic sequence (fault planes are from geological data discussed in the text); note that the maximum ground shaking lies within the hanging wall block of the faults and is not symmetric to the fault trace as predicted by the hazard scenario.

One of the limitations of 2D source models can be seen in the symmetric distribution of the ground shaking compared to the fault trace in the seismic hazard scenario of Figure 1a. This symmetry is not realistic, considering that in the Apennines of Italy the seismogenic sources are not vertical, but inclined normal faults. Several cases, including the recent 1997 Colfiorito earthquake sequence in the Umbria-Marche region (Amato et al., 1998), clearly show that during normal faulting earthquakes the maximum ground shaking occurs at the hanging wall of the fault, being controlled by the 3D fault geometry (Figure 1b).

The map distribution of the expected ground shaking is only one of the aspects that might be improved by introducing the 3D geometry of seismogenic sources in models of PSHA. The 3D geometry of faults might allow us to better constrain the maximum area that can be ruptured by the earthquake. Consequently, more constraints on the seismogenic potential of the source might be introduced. The importance of the source area on the seismogenic potential of a structure is clearly expressed by the definition of the scalar seismic moment (M_0), the most physically meaningful parameter for measuring the earthquake size. Actually, M_0 is directly proportional to the fault area (A), according to the well-known equation $M_0 = GDA$ (G = shear modulus; D = average coseismic displacement). Therefore, any effort towards a better definition of the area of the active faults (i.e. the 3D geometry) is an effort towards a better definition of the associated sismogenic potential.

The degree of knowledge on active tectonics and seismicity of Italy is sufficiently high to attempt the definition of models of seismogenic sources that take into account the geometry of faults at depth (3D seismogenic sources). In this work, we focus our attention on the Umbria-Marche-Abruzzo Apennine belt of central Italy and we propose a model of 3D seismogenic sources. Along the belt, an interdisciplinary study is possible thanks to the availability of a large number of detailed surface and sub-surface geological–geophysical data. We also propose a

methodological procedure in defining 3D seismogenic sources and the associated seismogenic potential (i.e. the maximum expected magnitude), which is rather new compared to previous seismotectonic studies in Italy.

Our approach is mainly structural-seismotectonic. We integrate surface geology data with seismological and subsurface structural data in order to identify active faults and to define: (i) the deep geometry of the fault structures; (ii) the segmentation pattern; (iii) the down-dip extent of the seismogenic faults (thickness of the brittle layer and/or termination on detachment faults); (iv) the seismic behaviour and seismogenic role (e.g. activation during previous earthquakes); (v) the structural style of the active deformation at a wider scale; and (vi) a model of sources (seismogenic boxes) that can be directly used for regional-scale seismic hazard simulations.

Surface expression of active faults: A brief review

The Apennines of central Italy are affected by Quaternary normal faulting tectonics (Figure 2) (Calamita and Pizzi, 1994; Lavecchia et al., 1994; Barchi et al., 2000; Boncio et al., 2000; Galadini and Galli, 2000; Galadini et al., 2000; Pizzi and Scisciani, 2000; Valensise and Pantosti, 2001; Lavecchia et al., 2002 and references therein). Normal faults have NNW-SSE average strike; they mainly dip towards WSW and display

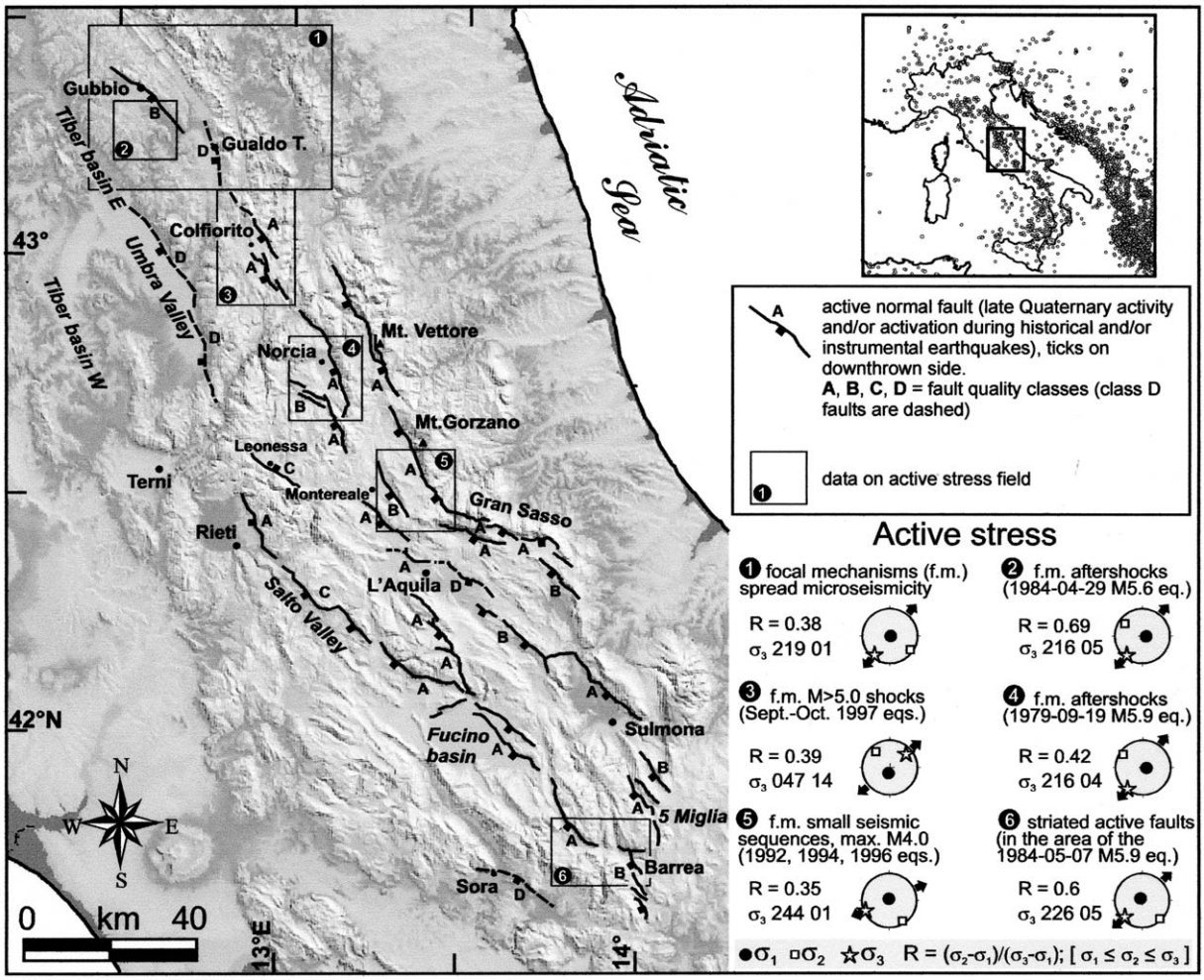

Figure 2. Digital elevation model of central Italy with active normal faults of the Umbria-Marche-Abruzzo Apennines and parameters of active stress tensors obtained by inversion of focal mechanisms of background microseismicity (1), aftershock sequences (2, 3, 4, 5) or striated active faults in seismic areas (6); stress data from Brozzetti and Lavecchia (1994), Boncio and Lavecchia (2000a) and Pace et al. (2002a); the stress axes are given as trend (first three numbers) and plunge (last two numbers).

dip–slip to normal–oblique kinematics. Ongoing extension driven by nearly horizontal NE-trending deviatoric tension is confirmed by fault slip data on active faults as well as by earthquake focal mechanisms (Figure 2, Table 1; Brozzetti and Lavecchia, 1994; Frepoli and Amato, 1997, 2000; Boncio and Lavecchia, 2000a). Only a limited number of Authors consider that the Quaternary deformation is dominated by strike–slip regime (e.g. Cello et al., 1997), but geological and seismological evidence for strike–slip deformation is weak.

An active fault of interest for seismic hazard assessment is a structure that has an established record of activity in the late Quaternary (i.e. in the past 125 kyr) and a demonstrable or potential capability of generating major earthquakes (see Machette, 2000 for a discussion on terminology). The active faults compiled in this work are shown in Figure 2. Fault parameters are from both our updated work and from a revision of published fault compilations (Barchi et al., 2000; Galadini et al., 2000; Valensise and Pantosti, 2001 and references therein); we also used information from recent detailed geologic maps (Vezzani and Ghisetti, 1998; 1:50000 unpublished maps of central-northern Abruzzo Apennines: *Avezzano*, *Sulmona* and *L'Aquila* sheets and related explanatory notes).

The faults undertake one or more of the following requirements: (1) evidence of activity in late Quaternary times; (2) paleoseismological evidence; and (3) activation during instrumental seismic sequences and/or association to historical earthquakes.

The faults of Figure 2 do not have the same quality, in terms of amount and type of data about the late Quaternary activity. We classified the active faults into four classes (A, B, C and D; fault classification modified from Galadini et al., 2000). Class A includes faults having clear evidence of repeated displacement episodes during the late Quaternary, as well as quantitative information on slip rate by specific paleoseismological and/or morphotectonic analyses. Class B includes faults having clear evidence of late Quaternary activity but quantitative data on fault slip rate is lacking (only qualitative estimates may be available). Class C includes 'debated' faults, which are faults described as active by some Authors, sometimes with quantitative information on late Quaternary slip rate, and as inactive by other Authors. Class D includes the less constrained structures, that are faults having poorly constrained geometry and longitudinal continuity and/or doubtful seismogenic role; their presence in the map of Figure 2 is motivated by the occurrence of significant seismicity, likely associated to the fault, and by regional-scale geologic considerations.

Except for faults of class D, the geometry and kinematics are constrained by structural–geological field data. The along-strike extent and segmentation pattern at surface are constrained by structural observations such as: (i) fault plane continuity in the field; (ii) presence of major fault irregularities interrupting the fault; (iii) identification and analysis of displacement of stratigraphic markers; (iv) major tectonic features, such as the control over sedimentation (fault-bounded basins).

The active faults are spread along three main alignments (Figure 2). The eastern alignment extends from Mt. Vettore to Mt. Gorzano and Gran Sasso; the intermediate alignment extends from Gubbio to Gualdo Tadino, Colfiorito, Norcia, Montereale, L'Aquila, Sulmona and 5 Miglia; the western alignment extends from Umbra Valley to Rieti, Salto Valley, Fucino and Barrea.

Debated and doubtful structures

Debated faults are the NE-dipping Leonessa and the SW-dipping Salto Valley faults. The Leonessa structure is described as an active normal fault by Michetti and Serva (1990) and Cello et al. (1997), who estimated an average throw rate of 0.1–0.4 mm/yr; nevertheless, in recent fault compilations (Galadini et al., 2000), the Leonessa fault is considered active only during the Quaternary before late Pleistocene and inactive during late-Quaternary times. The Salto Valley fault is a Plio-Quaternary normal fault considered active by Morewood and Roberts (2000), who calculated throw rates of 0.22–0.56 mm/yr for the last 18 kyr. Clear evidence of late-Quaternary displacements is present in the central portion of the fault (Fiamignano strand; Bosi, 1975; Galadini and Messina, 2001). Nevertheless, this evidence has been interpreted as due to deep-seated gravitational movements, rather than to tectonic displacement, by Galadini and Messina (2001) who consider the Salto Valley fault as inactive.

The most doubtful structures, in terms of longitudinal continuity and seismogenic role, are the Umbra Valley, Gualdo T., east of L'Aquila and Sora structures (class D, dashed faults in Figure 2), for the lack of clear surface evidence of the fault plane. The recent-to-present activity of these normal faults is suggested by the occurrence of significant historical earthquakes (Gualdo T., Umbra Valley, L'Aquila and Sora earthquakes; Working Group CPTI, 1999; see also

Table 1. Geometric and kinematic parameters of the seismogenic master faults of Figure 3. The attitude at surface (str. = fault strike; dip = dip direction; incl. = inclination) is given as average values or range of values; L = along-strike length; W = down-dip length (# = average inclination assumed to be 50°), W_s = width of the surface projection of the fault plane (coinciding with the box width of Figure 9); D = thickness of the seismogenic layer (from: EQ = earthquake data; SR = seismic reflection data; R = rheological profiling). Stress tensors are obtained by inversion of kinematic indicators on the master fault and associate subsidiary structures; the stress axes are given as trend (first three numbers) and plunge (last two numbers); (+) = structure of doubtful longitudinal continuity or seismogenic role (class D fault). References for kinematics and stress data (this work if not specified): MT91 = Marsili and Tozzi (1991); C89 = Cavinato et al. (1989); C1 = Calamita et al. (2000a); C2 = Calamita et al. (2000b); C97 = Cello et al. (1997); B99 = Basili (1999)

		Attitude at surface (°)			Dimensions (km)					Stress tensor			
N°	Master fault	str.	dip	incl.	L	W	W_s	D	kinematics	$\sigma 1$	$\sigma 2$	$\sigma 3$	Ref.
1	Mt. Bove–Mt. Vettore	140–170	SW	60	35	19.5#	12.5	15 (R+EQ)	dip slip	30278	14210	05104	
2	Mt. Gorzano	150–160	SW	50–70	28.5	19.5#	12.5	15 (EQ+R)	dip slip	23484	32601	05606	MT 91
3	Gran Sasso	090–120	S-SSW	40–70	28.5	19.5#	12.5	15 (EQ+R)	dip slip/ transt. dx	max extension NNE			C2
4	Gubbio	130	SW	50	23.5	12	10	6 (EQ+SR)	dip slip	04480	14200	23210	
5	Gualdo T. (+)	170	WSW	/	19	14	11	8 (SR)	/	/	/	/	
6	Colfiorito	145	SW	55	19	14	10	8–9 (EQ+SR)	dip slip	07865	33506	24224	C1
7	Cesi–Mt. Civitella	145	SW	60	14	10	8	6–7 (EQ+SR)	dip slip	35179	10104	19210	C1
8	Norcia (Nottoria-Preci)	135–180	SW-W	50–75	29	15.5	10	12 (EQ)	dip slip/ transt. sx	17169	33320	06505	
9	Cascia–Cittareale	115–160	SW	60–75	24	17.5#	11.5	12–15 (EQ+R)	dip slip/ transt. sx	04888	14201	23202	
10	Montereale	145–120	SW-SSW	60	16	19.5#	12.5	15 (EQ+R)	dip slip/ transt. dx	12773	31016	22001	B99
11	Pizzoli–Mt. Pettino	100–130	SSW-SW	60–70	24	19.5#	12.5	15 (R)	dip slip/ transt. dx	15968	30218	03612	C97 B99
12	Aquilano *s.l.* (+)	150	SW	/	13	19.5#	12.5	15 (R)	/	max extension NE			
13	Middle Aterno Valley	120–130	SW	50–70	24	19.5#	12.5	15 (R)	dip slip	max extension NNE			C2
14	Sulmona	130–140	SW	40–50	23.5	19.5#	12.5	15 (R)	dip slip	max extension NE			
15	Mt. Pizzalto–5 Miglia	140–160	SW	70–80	18	19.5#	12.5	15 (R)	dip slip/ transt. sx	max extension NNE			
16	Umbra Valley north (+)	145–180	SW-W	/	28.5	5–6	4	4–5 (EQ+SR)	dip slip/ transt. sx	/	/	/	
17	Umbra Valley south (+)	145–180	SW-W	/	24	5–6	4	4–5 (EQ+SR)	dip slip/ transt. sx	/	/	/	
18	Rieti	140–160	WSW	80	16.5	13#	8.5	10 (R)	dip slip	max extension NE			C89
19	Salto Valley	090–150	S-SW	45–70	28.5	14.5#	9	10–12 (R)	dip slip	22382	32101	05107	
20	Mt. Velino–Magnola	100–130	SSW-SW	35–55	26.5	16.5#	10.5	12–13 (R)	dip slip	max extension NE			
21	Campo Felice–Ovindoli	125–170	SSW-SW	45–80	26.5	17#	11	13 (R)	dip slip/ transt. sx	08572	32708	23515	
22	Fucino	140	SW	55–65	25	17#	11	13 (R)	dip slip				
23	Mt. Marsicano	110–140	SW-SSW	60–75	21	17#	11	13 (R)	dip slip/ transt. sx	32084	11806	20802	
24	Barrea	140–160	SW	60	17.5	17	11	13 (EQ+R)	dip slip	03985	13601	22605	
25	Sora (+)	130	SW	/	20	14.5#	9	11 (R)	/	/	/	/	

Figure 10), by a few seismic reflection data coupled with instrumental seismicity (e.g. Gualdo T.; Boncio et al., 1998), as well as by their imprinting on the morphologic and sedimentary evolution of the hanging wall block during Quaternary times.

Segmentation model and 'seismogenic master faults'

An important step in defining a model of seismogenic sources is the definition of a segmentation model significant for PSHA. In this work, we define a 'static' segmentation model, based on geological data, locally integrated with observation of past earthquakes. We call 'seismogenic master faults' those major structures that can be considered substantially continuous at depth for several kilometres, even if in some cases they are segmented at the surface in closely spaced structures of minor hierarchical order (Figure 3).

In the map of Figure 3, the Leonessa normal fault is not considered a master fault. It is due to the fact that the NE-dipping Leonessa fault and the SW-dipping Cascia-Cittareale fault (N° 9) intersect at depth, within the seismogenic layer (12–15 km thick, see Table 1 and the discussion in the following section). These structural relations may be interpreted as: (1) one fault is a subsidiary structure, antithetic to the other; (2) one fault is an older structure cut by the younger one. In both cases only one of the two faults can be considered as master fault. Considering that the Leonessa structure is a class C fault (debated structure), we considered only the Cascia-Cittareale structure as master fault.

The seismogenic master faults are separated from each other by first-order structural or geometrical complexities, e.g. complexities of kilometric dimensions (Figures 3 and 4). The first-order complexities considered here consist of mainly 3 types: (1) 3–4 km fault gaps among aligned structures (G in Figure 3); (2) sharp bends or intersections with cross structures (often transfer faults) extending 4–9 km along strike and oriented at nearly right angles with intersecting faults (B-I in Figure 3); (3) overlapping or underlapping *en échelon* arrangements (i.e. stepovers, S in Figure 3) with separations between faults ranging from 2 to 5 km.

Closely spaced minor fault strands, such as those of structure 7 in Figures 3 and 4 (separated by hundreds of metres complexities), are considered not able to seriously interrupt the continuity of the master fault at depth. Large single faults displaying the features of large isolated segments (on the basis of displacement profiles) are considered as master faults. In Figure 5, we show the example of the Mt. Gorzano normal fault.

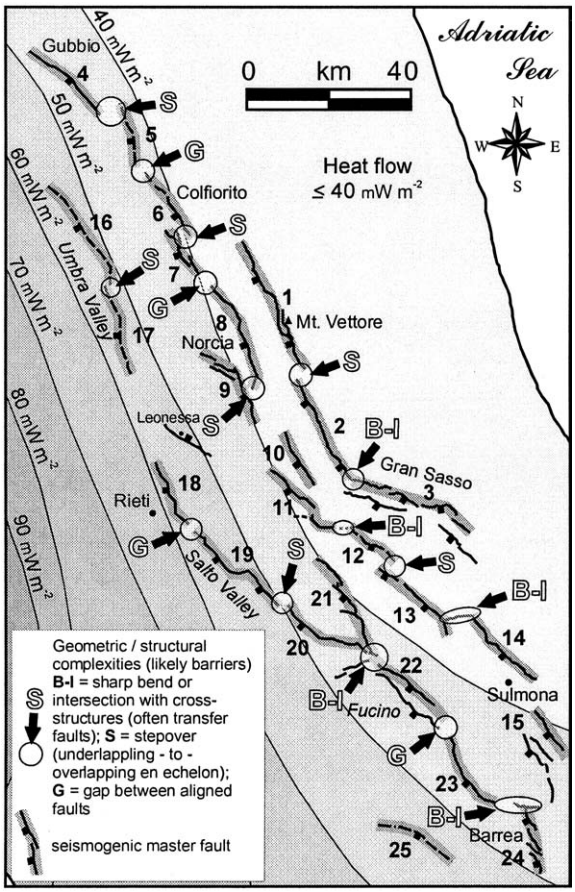

Figure 3. Proposed segmentation model illustrating the seismogenic master faults (thick grey lines, see text for definition) and the geometric–structural complexities (likely barriers) separating them; numbers near the master faults coincide with numbering in Table 1; the regional pattern of surface heat flow (from Pasquale et al., 1997) is indicated.

Field evidence and stratigraphic displacements allow us to identify an isolated fault segment extending about 28 km along-strike; it is delimited by two major fault irregularities: a stepover with the northern Mt. Vettore fault (the separation is 3 km), and an intersection with a nearly-orthogonal structure to the south (the Gran Sasso fault). In Figure 5, it is also highlighted the fault portion for which evidence of late-Quaternary activity is clearly documented from morphotectonic analyses (Galadini and Galli, 2000). The fault portion with clear late-Quaternary activity is shorter than the structurally-defined fault segment, identified by the analysis of fault plane continuity and stratigraphic displacements; it is a feature common to many faults considered in this work (compare fault parameters compiled in Barchi

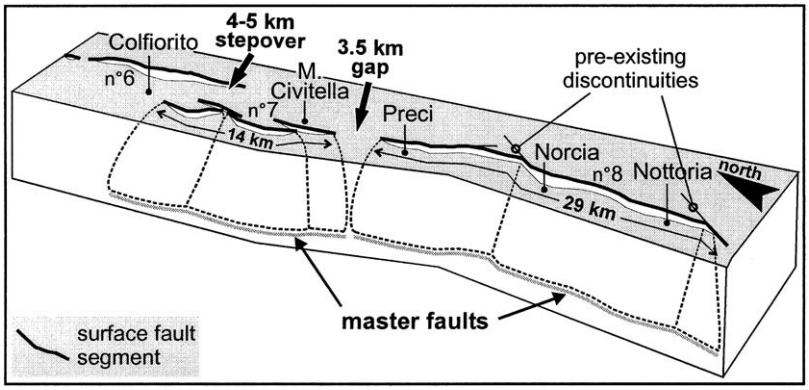

Figure 4. Schematic block diagram illustrating the concept of master faults (major fault structures substantially continuous at depth) and major complexities separating them; the numbering coincide with Figure 3 and Table 1; the surface lengths of the master faults N° 7 (Cesi–Mt. Civitella, 14 km) and N° 8 (Norcia, 29 km) are indicated.

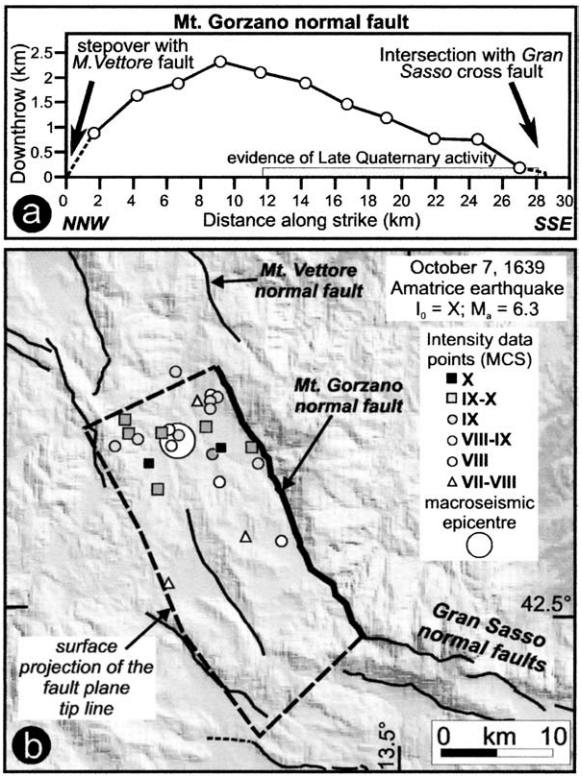

Figure 5. (a) Displacement profile along the Mt. Gorzano normal fault (fault N° 2 in Figure 3) built by measuring the offset of stratigraphic markers on geological cross sections; the fault portion having clear evidence of late-Quaternary activity (from Galadini and Galli, 2000) is highlighted; (b) MCS intensity data points (I≥VII–VIII from DOM 4.1 database; Monachesi and Stucchi, 1997) for the 1639 Amatrice earthquake, associated to the Mt. Gorzano fault (northern portion); the fault pane is constrained by geological, seismological and rheological data discussed in the text.

et al., 2000). Commonly, the fault portion showing clear evidence of late-Quaternary displacements is considered as the expression of the surface rupture of the maximum earthquake; its length is often used in order to derive the maximum expected magnitude through empirical relations (Mw from surface rupture length, SRL; Wells and Coppersmith, 1994). The divergence between structurally-defined and morphotectonically-defined fault lengths can be explained by considering that the maximum expected earthquake, able to break the whole seismogenic layer, may rupture at surface a fault portion much shorter than the total fault length at depth (sub-surface rupture length); the 1997 Colfiorito earthquake sequence in the Umbria-Marche Apennines is an example (e.g. Cinti et al., 2000). The statistical analysis by Wells and Coppersmith (1994) indicates that for normal faulting earthquakes, rupturing the whole seismogenic layer, the sub-surface rupture length (RLD) is longer than the surface rupture length (SRL) up to 35–45%. Therefore, it is suggested that the structurally- and morphotectonically-defined fault lengths are not conflicting but complementary quantities. The identification of late-Quaternary displacements along faults is a necessary ingredient in defining the fault activity, but it is not sufficient in fully describing the fault geometry and segmentation pattern. The combination of morphotectonic observations with structural reconstructions may give a more realistic picture of the 3D seismogenic source.

Although the identification of boundaries between earthquake segments (segments which may be activated by a single rupture episode) is far from being straightforward (see McCalpin, 1996 pp. 467–475 for

a review and discussion), we assume that the structural–geometrical complexities previously described are likely able to stop the rupture propagation of the largest expected earthquake (likely barriers). Therefore, they are considered as boundaries between major earthquake segments. Our segmentation model does not exclude the possibility that adjacent master faults might interact with each other at the time of an earthquake, producing triggered events (e.g. through stress variations; Das and Scholz, 1981; King et al., 1994).

The master fault segments identified by these criteria range in length from 13 to 35 km. The main geometric and kinematic parameters of the seismogenic master faults are listed in Table 1.

Constraining the 3rd dimension by integrating surface and subsurface data

The shape and dimension of the seismogenic fault plane cannot be constrained by knowing only the fault pattern at surface: the geometry at depth may be listric or planar; the depth extent of faults may vary depending on the tectonic and thermal context (e.g. presence of a detachment fault and/or transition from brittle to plastic behaviour). In Figure 6, three simplified situations in which the structural style of the extensional deformation may influence the area of the seismogenic fault are sketched. Therefore, the consideration of the third dimension is essential and the map pattern must be integrated with subsurface geological/geophysical data. The subsurface data considered in this work consists of available seismic reflection–refraction profiles (and specific works on geologic interpretation), well constrained location of earthquake hypocentres and thermo-mechanical properties of crustal rocks (Figures 3, 7 and 8). All the data contribute to constrain the thickness of the seismogenic layer, the down-dip length and, in some cases (e.g. seismic reflection profiles, well-located aftershock sequences), the down-dip geometry of fault planes. Fault parameters in the 3rd dimension, including the data used in constraining them (seismic reflection data, earthquake data, rheology or combined) are summarised in Table 1.

Deep geological–geophysical prospecting data

The central Apennines are crossed by two seismic refraction profiles (DSS profiles): the northern one is the most detailed one and crosses the Umbria-Marche Apennines (DSS Piombino-Ancona, Ponziani et al., 1995); the southern one crosses the Abruzzo Apennines (DSS Latina-Pescara, Scarascia et al., 1994). DSS data help to reconstruct the crustal layering, the related seismic velocities, the likely densities and the inferable main composition (e.g. Rudnick and Fountain, 1995). DSS data, integrated with seismic reflection profiles and surface geology is useful in defining velocity models for earthquake location, as well as in constraining the crustal layering for rheological models. Three main crustal layers can be identified beneath the Apennine extensional area from DSS data. From top they are: (1) the sedimentary cover, 4–6 km thick, consisting

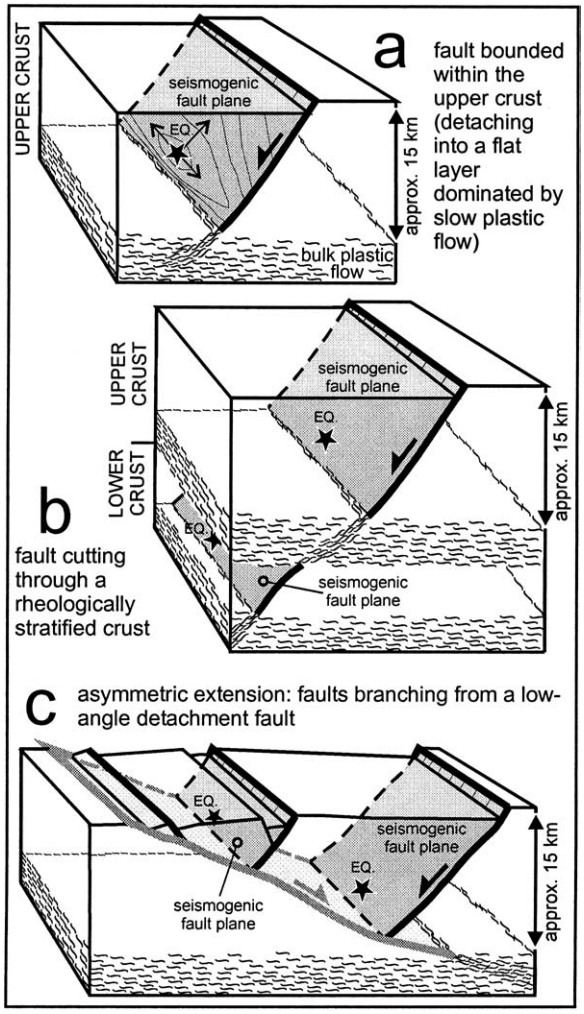

Figure 6. Schematic block diagrams illustrating different structural settings influencing the extent at depth of the seismogenic plane for active normal faults; the focus of the expected earthquake (EQ), denoted by a star, and the direction of the rupture propagation are qualitatively indicated.

of siliciclastic turbidites, not ubiquitously distributed (average P-wave velocity Vp = 4.0 km/s, average density ρ = 2400 kg/m^3), carbonates (Vp from 5.5 to 6.0 km/s, ρ = 2500 kg/m^3) and anhydrites (Vp = 6.2 km/s, ρ = 2510 kg/m^3); (2) an intermediate layer, 10–12 km thick, consisting of quartzites and phyllites (upper part; Vp = 5.0-5.2 km/s, ρ = 2620 kg/m^3) and mid-crustal rocks of likely felsic composition (Vp from 6.3 to 6.0 km/s, ρ = 2650 kg/m^3); 3) a lower-crustal layer, 15–22 km thick, of likely intermediate-to-mafic composition (Vp from 6.7 to 6.5 km/s, ρ = 2850 kg/m^3).

Seismic reflection profiles, integrated with surface geology and borehole data give important constraints on the deep geometry of faults and the structural style of the deformation. Significant constraints from reflection profiles are available for the northern sector (Umbria-Marche Apennines, Figure 7; Barchi et al., 1998; Boncio et al., 1998; Collettini et al., 2000), while in the southern sector comparable constraints are lacking. In the Umbria-Marche Apennines, seismic reflection data show important structural features: the extension is asymmetric and the major active SW-dipping normal faults terminate at depth on a low-angle NE-dipping extensional detachment fault (the Altotiberina fault, AF in Figure 7). In Figure 7, three geological sections derived from interpretation of seismic reflection profiles illustrate this structural feature. These sections also show a listric geometry of the SW-dipping active normal faults detaching onto the AF. The AF detachment is a structure of regional importance, extending for dozens of kilometres along-strike (for details see Boncio et al., 2000); the depth of the AF ranges from 4–5 km in the western side of the Umbria-Marche

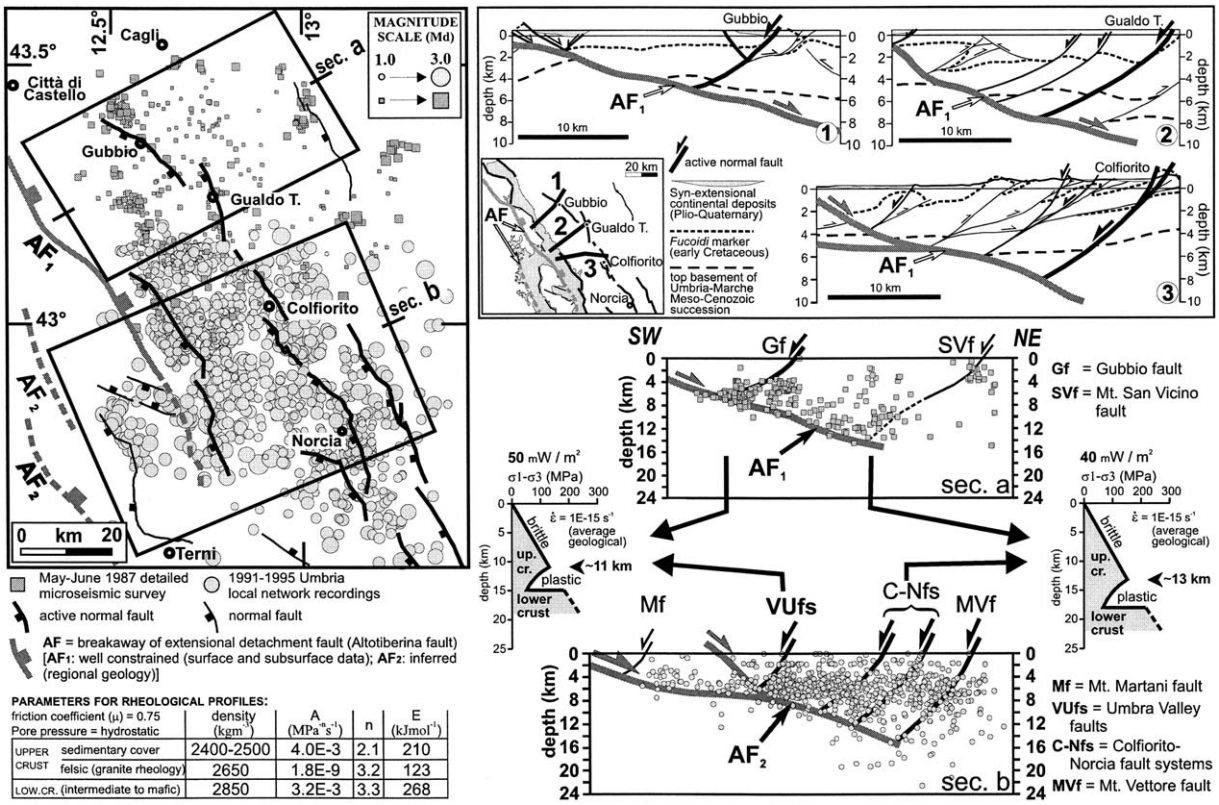

Figure 7. Geological cross sections from seismic reflection profiles across the Gubbio, Gualdo T. and Colfiorito seismic areas (from Boncio et al., 1998; Boncio and Lavecchia, 2000b); epi- and hypocentral distribution of back-ground microseismicity recorded in the Umbria-Marche Apennines and rheological profiles (strength envelopes in critical stress difference, σ_1–σ_3) built for two different thermal contexts (50 and 40 mW/m^2 surface heat flow, see Figure 3 for location); the depth of the brittle-plastic transition on rheological profiles is indicated by arrows; the used rheological parameters are indicated: crustal layering is from DSS data; A (empirical material constant), n (stress exponent) and E (activation energy) are creep parameters; $\dot{\varepsilon}$ = longitudinal strain rate (calculated by balancing of a regional geologic section; Figure 5 in Boncio et al., 2000); see text for further details.

Apennines (Umbra Valley) to 12–14 km beneath the axial zone of the Apennines. This is of particular importance for our purposes, because the down-dip length of the active faults is controlled by the relative position within the AF hanging wall; it increases moving from west to east. Under the same fault length, the fault area increases accordingly.

In the southern area (Abruzzo Apennines), the short availability of subsurface structural data (e.g. seismic lines) does not permit to have a detailed structural view as in the Umbria-Marche Apennines. Up to now, there is no data on the presence or depth of the AF detachment fault, which can be reasonably traced as far as the southern termination of the Tiber basin (Figure 7, Boncio et al., 2000). Due to the lack of such information, sub-surface data for the Abruzzo Apennines is limited to instrumental earthquake data and rheological rock properties discussed in the next sections.

Detailed earthquake data

The instrumental seismicity data represent a good chance to look at seismogenic processes. They provide basic information on the thickness of the seismogenic layer and geometry of the deforming rock volumes. At present, data having sufficient detail to be used for seismotectonic purposes derive from recent microseismic activity and from a number of small ($3.0 < M < 5.0$)- to - moderate ($5.0 \leq M \leq 6.0$) earthquake sequences (Figures 7 and 8).

In Figure 7, the background microseismicity recorded in the Umbria-Marche area is shown. Two datasets are reported: (1) the 1987 records of a dense temporary network ($0.5 \leq M \leq 3.1$, errors $\leq$2.5 km; Deschamps et al., 1989; Boncio et al., 1998) and (2) the 1991–95 records of the Umbria regional network ($1.0 \leq M \leq 3.7$, errors $\leq$2.0 km; Boncio et al., 1998). The latter database is not as well constrained as the former, but both databases indicate a first-order feature: an east-deepening of the seismicity cut-off, from $\sim$6 km in the western side to 14–15 km in the eastern side. This eastward deepening of the hypocentres is consistent with the geometry of the AF detachment fault shown by seismic reflection profiles, indicating that deformation is mainly located within the hanging wall block of the AF. This implies that the seismicity cut-off is primarily controlled by a structural feature (a detachment fault). The E-deepening of the seismicity cut-off is unlikely related to lateral variations of rock rheology, as indicated by strength profiles (see the following section), reinforcing the conclusion that it is structurally controlled.

In Figure 8, the epi- and hypocentral distribution of recent earthquakes and related aftershock sequences are shown. From north to south they are: the Gubbio 1984 (M_w 5.6), Colfiorito 1997 (maximum M_w 6.0), Norcia 1979 (M_w 5.9), north L'Aquila area 1992, 1994 and 1996 (maximum M_d 4.0) and Sangro 1984 (maximum M_w 5.9) earthquakes (Deschamps et al., 1984; Haessler et al., 1988; Amato et al., 1998; Boncio and Lavecchia, 2000a, 2000b; Cattaneo et al., 2000; De Luca et al., 2000; Pace et al., 2002a; Boncio et al., 2004). All the main shocks have normal or normal–oblique kinematics and ruptured faults, or portion of faults, exposed at surface. Evidence of coseismic surface breaks, not unanimously interpreted as surface faulting, is documented only for the 1997 Colfiorito earthquake sequence (Cello et al., 1998; Basili et al., 1998; Cinti et al., 2000). The maximum depth of the activated seismogenic faults, as deduced from aftershocks, is 6–7 km for the Gubbio structure, 8–9 km for Colfiorito, 11–12 km for the Norcia structure, 14–16 km for the Mt. Gorzano structure and 13–14 km for the Barrea fault in the Sangro area.

Heat flow and thermo-mechanical properties of crustal rocks

In analysing the thickness of the brittle layer, we compared instrumental seismological data with the first-order strength and behaviour (brittle versus plastic) of the crust estimated by rheological profiling (Ranalli and Murphy, 1987). Brittle strength can be estimated by calculating the critical stress for frictional failure along existing faults (Sibson, 1974; Byerlee, 1978); plastic strength can be estimated by the critical stress necessary for rocks to exhibit slow steady-state flow (most commonly dominated by power-law creep; Kirby, 1983). At a given depth, rocks deform in a brittle or plastic manner according to which strength is the lowest. At a first approximation, it is expected to observe consistency between brittle layers and location of earthquake hypocentres, while plastic layers should remain relatively aseismic. The crustal strength-behaviour was obtained by rheological profiling under the observed: (i) tectonic regime (normal faulting); (ii) strain rate (geologic and geodetic strain rates are considered); (iii) crustal layering and inferable rheological parameters (mainly from DSS data); and (iv) thermal field. The parameters used for rheological profiles are indicated in Figure 7. The geotherms were

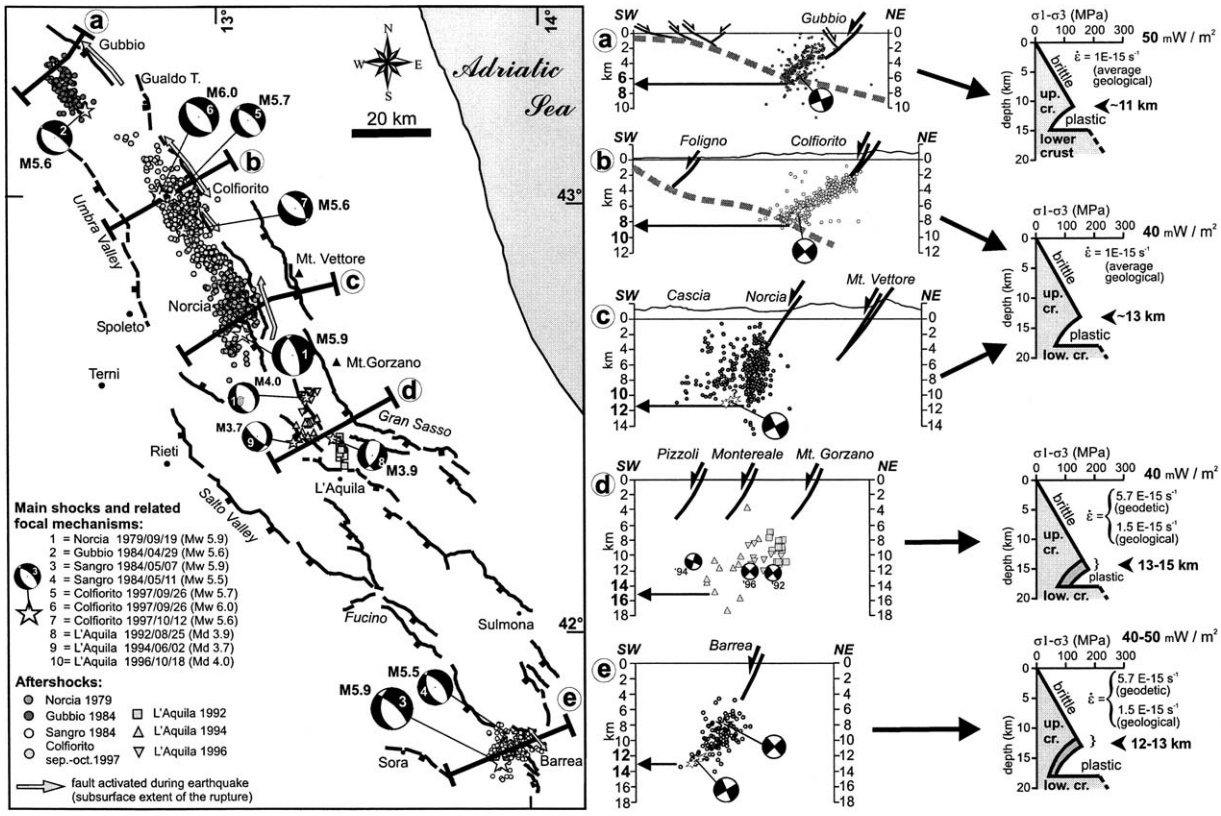

Figure 8. Epicentres of the major seismic sequences of the last twenty years (Gubbio, 1984; Colfiorito, 1997; Norcia, 1979; Sangro, 1984) plus three small seismic sequences in the L'Aquila area (1992, 1994 and 1996); seismotectonic sections and rheological profiles built according to the local thermal context. The dashed line (sections 'a' and 'b') represents the AF low-angle extensional detachment; arrows in seismotectonic sections indicate the maximum depth-extent of the activated seismogenic faults as suggested by the best defined aftershock volume; rheological parameters as in Figure 7; in the southern Abruzzo area, creep strengths for geologic and geodetic longitudinal strain rates are compared (geologic strain rate calculated from data of Galadini and Galli, 2000; geodetic strain rate from D'Agostino et al., 2001); seismological data from Amato et al. (1998); Boncio (1998); Boncio et al. (2004); Cattaneo et al. (2000); De Luca et al. (2000); Deschamps et al. (1984); Ekstrom et al. (1998); Haessler et al. (1988); Harvard CMT database at *www.seismology.harvard.edu*.

computed under the assumption of steady-state thermal regime, by using the regional surface heat flow (ranging from 60 to 40 mW/m^2, Figure 3; Pasquale et al., 1997) and considering an exponential decrease of heat production for basement rocks underlying the sedimentary cover (thermal parameters from Dragoni et al., 1996).

In Figures 7 and 8 the rheological profiles are compared with the depth distribution of seismicity. We observe that in several cases the seismicity cut-off at depth and the brittle-plastic transition from rheological profiles are in good agreement. Obviously, the brittle–plastic transition must be considered as a broad zone, rather than a sharp boundary. In the eastern Umbria-Marche Apennines (eastern profile in Figure 7, at 40 mW/m^2), both the rheology and seismicity cut-off suggest that active structures detach at mid-crustal levels (13–15 km depths) into a layer dominated by aseismic plastic flow. Similar conclusions can be drawn for the seismic zones in the northern L'Aquila area (brittle-plastic transition at 13–15 km depths and seismicity cut-off at 14–16 km, section 'd' in Figure 8) and in the Barrea area (brittle-plastic transition at 12–13 km depths and seismicity cut-off at 13–14 km, section 'e' in Figure 8). It is suggested that rheological profiling may be a powerful tool in estimating the seismogenic layer thickness; this information could be used for those areas where detailed seismological data are lacking but the surface heat flow, crustal layering and strain rate are known.

Disagreement between seismicity cut-off and brittle-plastic transition from rheology is observed in the western area of the Umbria-Marche Apennines (western profile in Figure 7, at 50 mW/m^2; profiles 'a'

and 'b' in Figure 8). The observed disagreement can be explained by considering that in this area the seismicity cut-off is not rheology-controlled, but it is structurally controlled by the AF detachment. In the Norcia seismic zone (profile 'c' in Figure 8), the seismicity cut-off (at ∼12 km) is located near the depth of the brittle-plastic transition inferred from rheology (∼13 km), but we do not exclude that also in this area the seismicity cut-off might be structurally-controlled by the AF detachment, similarly to the northern Colfiorito area. Unfortunately, there is no detailed sub-surface data to corroborate this hypothesis.

In constraining the seismogenic layer thickness, we use mainly the seismicity data, or seismicity coupled with seismic reflection data. Where these data are lacking, we use the seismogenic layer thickness inferred from rheological profiling, according to the local surface heat flow (Table 1).

From faults to seismogenic sources for PSHA applications

Seismogenic boxes

To give a plane view representation of the master faults, we introduce the term 'seismogenic box.' A seismogenic box is the surface projection of a seismogenic master fault (Figure 9), so it is different from the boxes obtained using macroseismic intensity data (e.g. Gasperini et al., 1999). The shape and dimension of each box strictly reflects the threedimensional geometry of the related master fault. The length of the box (L) is the along-strike length of the seismogenic fault, the width of the box (W_s) is the surface projection of the down-dip length (W). Ws is not constant in the area, being dependent on the inclination at depth of the seismogenic structure and on the depth of the local seismogenic layer (D). In Figure 10, we present a map of the seismogenic boxes of the Umbria-Marche-Abruzzo Apennines. The boxes are limited to the east by the surface trace of the related master faults and to the west by the surface projection of the intersection line (e.g. tip line) between the seismogenic fault plane and the base of the seismogenic layer.

To the seismogenic boxes, we can attach a quality class (from A to D), according to the quality classification of the related active faults.

The boxes having the largest W_s are those belonging to the easternmost alignment (N° 1, 2 and 3 in Figure 10), due to the relatively large depth of the local seismogenic layer (∼15 km), and the Gubbio box (N° 4), due to the low inclination at depth of the fault plane (compare Figure 7). The boxes having the smallest W_s are the Umbra Valley north (N°16) and Umbra Valley south (N° 17), due to the relatively small depth of the local seismogenic layer (4–5 km).

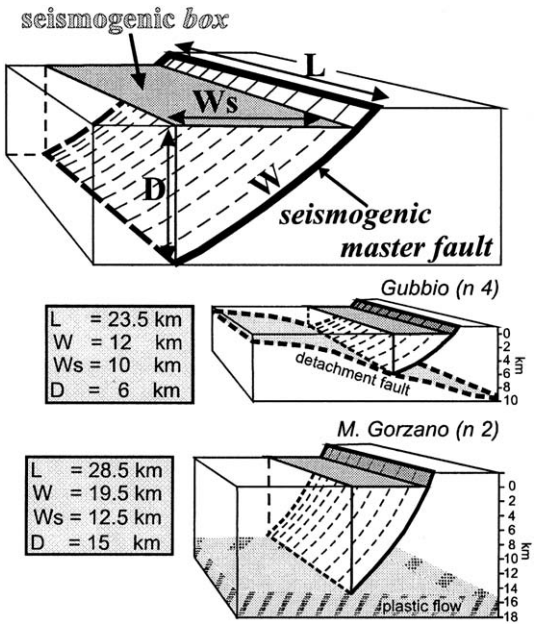

Figure 9. 3D representation of a seismogenic box: W_s = box width; L = along-strike length of the seismogenic master fault; W = down-dip length of the seismogenic master fault, D = thickness of the local seismogenic layer; the Gubbio and M. Gorzano examples are illustrated.

The simple polygonal shape of the boxes is due to a simplification of the true fault geometry; we consider this simplification as a compromise between clear observable features (along-strike length at surface) and non-measurable deep features of the fault (e.g. degree of ellipticity of the fault plane at depth; e.g. Walsh and Watterson, 1988).

The boxes are not simply a map representation of fault zones; they are the map projection of the radiating-energy sources significant for PSHA. The dimension of the boxes is proportional to the area of the seismogenic fault and, therefore, to the seismic moment predictable for the major earthquake on the fault. Within the boxes, the epicentres of each single major earthquake, as well as the maximum associated ground shaking, are expected to occur. Considering the kinematics of the master faults and the active stress field, the expected kinematics of the earthquakes within each source is normal

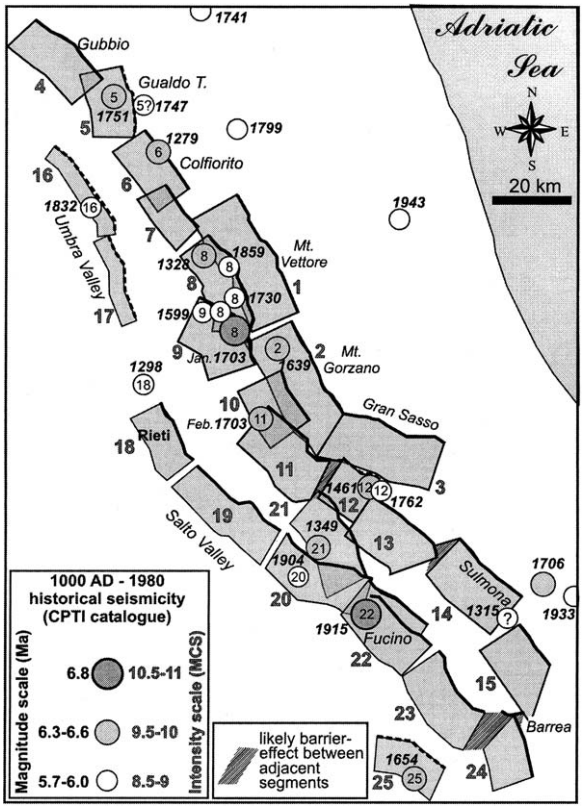

Figure 10. Map of the seismogenic boxes for the Umbria-Marche-Abruzzo Apennines and epicentres of historical earthquakes larger than VIII on the MCS scale (M ≥ 5.7) from C.P.T.I. catalogue (Working Group CPTI, 1999); dates refer to the year of earthquake occurrence; small numbers within epicentres coincide with the number of the associated box.

or normal–oblique with an average SW–NE trending slip vector.

The seismogenic boxes can be directly used for PSHA simulations at regional-scale, assuming that at this scale the true source inclination and geometry is negligible in terms of ground shaking response (Pace, 2001; Pace et al., 2002b; Peruzza and Pace, 2002).

Association of past earthquakes to seismogenic sources

Each fault alignment is characterised by a set of historical and/or instrumental earthquakes (Figures 8 and 10). The association of instrumental earthquakes is controlled by the distribution of the aftershock sequences of the last 20 years seismic events. The association of historical records is based on the analysis of the distribution of the highest intensity data points (DOM 4.1 database, Monachesi and Stucchi, 1997; see Figure 5b for an example) related to large earthquakes (I > VIII, $M \geq 5.7$). For all the historical earthquakes, the size is given in terms of epicentral intensity (I_0, MCS scale) and average magnitude (M_a), both reported in the C.P.T.I. catalogue (Working Group CPTI, 1999).

The eastern alignment consists of three sources with different characters of seismicity. The northernmost and southernmost sources (N° 1 Mt. Bove–Mt. Vettore and N° 3 Gran Sasso, respectively) are silent since historical times, but show paleoseismological evidence of strong pre-historic earthquakes (Galadini and Galli, 2000). The 1639 earthquake ($I_0 = X$), which seriously damaged the Amatrice area, may be associated to the central source (N° 2 Mt. Gorzano; Figure 5b), even if the earthquake dimension ($M_a = 6.3$) suggests that it did not activate the entire structure.

The intermediate alignment is the most seismically active. In the last 20 years, it has been interested by the earthquakes of Norcia 1979 ($M_w = 5.9$), Gubbio 1984 ($M_w = 5.6$) and by a long seismic sequence which lasted from September 1997 to April 1998 affecting the Colfiorito, Sellano and Gualdo T. areas (Colfiorito: September 26, 1997 $M_w = 5.6$ plus $M_w = 6.0$; Sellano: October 12, 1997 $M_w = 5.2$ and October 14, 1997 $M_w = 5.6$; Gualdo T.: April 03 1998 $M_w = 5.1$). The 1979 and 1984 earthquakes activated respectively the sources N° 8 (southern portion) and N° 4 (southern portion). The 1997–98 seismic sequence activated, with several rupture episodes, the source N° 6 and the southern portion of the N° 5 (September 1997 and April 1998 events, respectively) plus the source N° 7 (October 1997 events). As far as it concerns the historical seismicity, the distribution of the intensity data points suggests a number of associations, briefly summarised below from north to south (see also Galadini et al., 1999; Lavecchia et al. 2002).

The source N° 4 (Gubbio) has no historical earthquakes with $I_0 >$ VIII; only small-to-moderate earthquakes occurred in historical times, such as the April 1593 earthquake (I_0 = VII–VIII, $M_a = 5.3$).

The July 1751 earthquake ($I_0 = X$, $M_a = 6.3$) probably activated the all source N° 5 (Gualdo T.); the April 1747 earthquake ($I_0 = IX$, $M_a = 5.9$) lies slightly eastward of the same source, but its association cannot be excluded.

The April 1279 earthquake ($I_0 = X$, $M_a = 6.1$) may be tentatively associated to the source N° 6 (Colfiorito); the largest damages are shifted eastward compared to those related to the September 1997 earthquakes,

but this may result from the scarcity of the historical information.

The source N° 7 (Cesi–Mt. Civitella) has no historical earthquakes with $I_0 >$ VIII; only small earthquakes occurred in historical times, such as the April–August 1898 earthquakes (I_0 = VII, $M_a = 4.8$).

The source N° 8 (Norcia) has a number of associated events: December 1328 (I_0 = X, $M_a = 6.4$, northern portion activated); May 1730 (I_0 = VIII–IX, $M_a = 5.8$, southern portion activated); August 1859 (I_0 = VIII–IX, $M_a = 5.8$, northern portion activated). The same source was entirely activated by the first shock (January 14, 1703, I_0 = XI, $M_a = 6.8$) of the long 1703 seismic sequence, one of the most destructive of the central Apennines. The same shock probably triggered a rupture on the source N° 9 (Cascia–Cittareale). The seismic sequence 'moved' southward involving the source N° 10 (Montereale; January 16 shock; Stucchi, 1985) and, on February 2 (I_0 = X, $M_a = 6.7$), the source N° 11 (Pizzoli–Mt. Pettino) (Blumetti, 1995; Barchi et al., 2000).

The November 1599 earthquake (I_0 = VIII–IX, $M_a = 5.8$) probably activated the northern portion of source N° 9 (Cascia–Cittareale).

The November 1461 earthquake (I_0 = X, $M_a = 6.5$) and October 1762 (I_0 = IX, $M_a = 5.9$) may be tentatively associated to the source N° 12 (Aquilano *s.l.*), while the source N° 13 (Middle Aterno Valley) is considered to be silent during historical times.

An archaeologically inferred earthquake which affected the Sulmona town around the middle of the 2nd century AD (Galadini and Galli, 2001) could be related to the activity of the source N° 14 (Sulmona).

The December 1315 event (I_0 = IX, $M_a = 6.0$) is of uncertain location, and could be attributed to the sources N° 12 (Aquilano *s.l*) or N° 15 (Mt. Pizzalto–5 Miglia). Pantosti et al. (1996) suggest a possible correspondence between the 1315 event and a Middle Ages surface-faulting earthquake (occurred between 860 AD and 1400 AD) recognised by trench excavations along the Piano di Pezza strand of the source N° 21 (Campo Felice–Ovindoli). Nevertheless, this geology-constrained earthquake could also correspond to the September 1349 earthquake, which is another poorly constrained medieval event of the region.

The sources belonging to the western alignment are, in the northern sector, the most doubtful in terms of recent activity. Nevertheless, seismological data and, in one case, paleoseismological data (N° 18 Rieti; Michetti et al., 1995) indicate a seismogenic role of the alignment. There is a relatively large number of small-to-moderate earthquakes activating the sources N° 16 and 17 (Umbra Valley) such as the Foligno and the Spoleto earthquakes (at least eight earthquakes with VII $< I_0 <$ IX, $5.0 < M_a < 5.8$). The largest one is the January 1832 Foligno earthquake (I_0 = VIII–IX, $M_a = 5.7$) which probably resulted from the activation of the source N° 16 (Umbra Valley north).

The December 1298 earthquake (I_0 = VIII–IX, $M_a = 5.9$) has a doubtful location and can be tentatively associated to the source N° 18 (Rieti).

Moving towards south, the September 1349 earthquake (I_0 = IX–X, $M_a = 6.5$), of uncertain location, may be attributed either to source N° 19 (Salto Valley) or N° 21 (Campo Felice–Ovindoli). We prefer the association of the 1349 event to the Campo Felice–Ovindoli source; this event might correspond to the Middle Ages surface-faulting earthquake (860–1400 AD) recognised by trench excavations in the central portion of the source (Pantosti et al., 1996).

The February 1904 earthquake (I_0 = VIII–IX, $M_a = 5.5$) can be associated to the source N° 20 (Mt. Velino–Magnola).

The January 1915 Avezzano earthquake (I_0 = XI, $M_a = 7.0$) is surely associated to the source N° 22 (Fucino), based on geological, seismological and geodetic data (Michetti et al., 1996; Galadini and Galli, 1999; Ward and Valensise, 1989).

The source N° 23 (Mt. Marsicano) is considered to be silent during historical times, but it shows evidence of displacement during the late-Quaternary (Galadini and Galli, 2000; Barchi et al., 2000).

The July 1654 earthquake (I_0 = IX–X, $M_a = 6.2$) may be associated to the source N° 25 (Sora).

The only significant activity instrumentally monitored in recent decades along the western alignment is the May 1984 ($M_w = 5.9$) sequence, that ruptured the source N° 24 (Barrea) (Pace et al., 2002a).

Maximum expected magnitude

The immediate consequence of having recognised individual seismogenic structures, and having parameterised these structures using geological data, is the possibility to compute the maximum expected magnitude (M_{max}) on the basis of geometric–kinematic data, relatively independent from past earthquakes. The geometrical parameters we have used are the maximum along-strike length and the area of the seismogenic sources. The maximum rupture area has been calculated from the along-strike length (L) and the down-dip length (W) indicated in Figure 9.

Considerations on the dimensions of the rupture area, calculated from the aftershocks or estimated from the magnitude values of the historical earthquakes by applying scaling laws (e.g. Wells and Coppersmith, 1994), show that in most of the cases the considered earthquakes did not activate the entire source (i.e. the entire master fault), but smaller portions. An example is the 1979 Norcia earthquake ($M_w = 5.9$), which activated only part of the associated source (N° 8 Norcia, Figure 8). Nevertheless, considering that during the M 6.8 earthquake in January 1703, the whole source was probably activated by a single rupture episode, we suggest that the area of the whole master fault is, reasonably, the parameter which better gives estimates of the expected M_{max}.

The M_{max} (considered as moment magnitude, M_w) was calculated by using empirical and analytical methods (the results are compared in Figure 11). First, we calculated the M_{max} from the dimensions of the seismogenic sources (both source area and source length were considered) by applying the empirical relationships calibrated on normal faults by Wells and Coppersmith (1994).

The M_{max} was also calculated using analytical relationships between fault dimensions and seismic moment and between seismic moment and magnitude. For a rectangular source with area A, length L, width W, average displacement D and shear modulus G (here considered $3 \cdot 10^{10}$ Pa), the equation for scalar seismic moment ($M_0 = GDA$) may be expressed as:

$$M_0 = GDLW = GkL^2W \qquad (1)$$

where k is the strain drop, defined as the displacement to length ratio (D/L). In homogeneous seismotectonic regions, constant strain drop is a reasonable assumption (e.g. Scholz, 1990 and references therein). We use the value obtained by Selvaggi (1998), who found a nearly constant value of $k = 3 \cdot 10^{-5}$ for normal faulting earthquakes in the Apennines of Italy. After having computed an 'equivalent' seismic moment from the area of each source, we obtained the related magnitude (M_w) by using the relation:

$$M_w = (\log M_0)/1.5 - 10.73 \qquad (2)$$

The computed magnitude values, reported in Figure 11, range between 6.0 and 6.8. For each source, M_{max} shows oscillations due to the different used methods. Nevertheless, by considering that the errors associated to empirical relations is of the order of 0.2–0.3

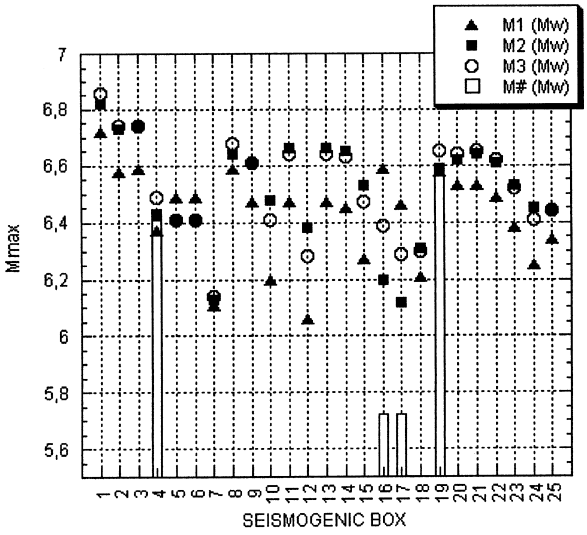

Figure 11. Maximum expected magnitude (M_{max}) calculated for each seismogenic source; $M1 = M_w$ from the length (L) of the master fault by using the Wells and Coppersmith (1994) empirical relations on subsurface rupture length (RLD); $M2 = M_w$ from the area of the master fault ($L \cdot W$) by using the Wells and Coppersmith (1994) empirical relations on rupture area (RA); $M3 = M_w$ from the scalar seismic moment calculated from the area of the master fault under the assumption of constant strain drop (equations 1 and 2); $M^{\#}$ = as for $M3$ but using $L^{\#}$ (calculated from equation 3) instead of L (see text for details); $M^{\#}$ is calculated only for those structures having $L > L^{\#}$.

points of magnitude, we can observe that the scatter is mainly within errors.

Although the M_{max} values obtained by different methods are comparable within the associated errors, our preferred estimates are those computed analytically from the fault area and the related 'equivalent' seismic moment ($M3$ in Figure 11). This procedure seems more coherent with our model, aimed to constrain the maximum area that can be ruptured by the expected earthquake.

Some not realistically large values of M_{max} were computed for the Umbra Valley sources (N° 16 and 17). These unrealistic estimates are due to the lack of constraints on the fault continuity along-strike, which allowed us to define sources relatively long (L = 23–31 km), but relatively narrow (W = 5–6 km). Assuming that the earthquake would rupture the whole fault area, this earthquake would have a relatively low value of the aspect ratio (W/L = 0.16–0.26), which sounds unrealistic if compared with the W/L values observed for earthquake normal faulting worldwide (Peruzza and Pace, 2002 and therein references). We examined the consistency between the expected W/L ratios of the

earthquakes expected on our source model and the observed W/L ratios for worldwide case studies by considering the results of Peruzza and Pace (2002). The Authors, examining the dataset used by Wells and Coppersmith (1994), implemented with the data reported in Vakov (1996) and Mai and Beroza (2000), computed a regression relationship to correlate the length of the possible maximum rupture (segment of fault that may be simultaneously broken, hereinafter indicated as $L^{\#}$) to its down-dip length (W, rather well constrained in our study region). The formula obtained for dip–slip earthquakes is:

$$L^{\#} = -2.3725 + 1.9354\mathrm{W} \quad R = 0.85 \qquad (3)$$

where R is the correlation coefficient the relationship, calibrated on about 180 events, has been applied in the Abruzzo Apennines test area (see Peruzza and Pace, 2002 for the complete description).

The value of $L^{\#}$ has been used to compute the $M^{\#}_{\max}$ values for those structures having length (L) larger than $L^{\#}$. The new values of $M^{\#}_{\max}$ have been calculated using the relations (1) and (2), without using the Wells and Coppersmith (1994) relationships. The $M^{\#}_{\max}$ values are plotted with white bars in Figure 11. Only for three sources (4, 16 and 17) the $L^{\#}$ value and the new $M^{\#}_{\max}$ differ substantially from the original values. This confirms that there is an acceptable consistency between our segmentation model and the earthquake scaling laws. The use of the $M^{\#}_{\max}$ may decrease significantly the importance of long structures such as the Umbra Valley sources (16 and 17).

Final remarks

Implications on PSHA

In this paper, we deal with the definition of a model of seismogenic sources constrained by geological–seismotectonic data and we apply this model to the Umbria-Marche-Abruzzo Apennines. Our model is useful for multidisciplinary PSHA that combines geological data with historical seismicity data, as suggested by methodologies developed recently (WGCEP, 1995; Frankel, 1995; Stirling et al., 2002). We propose that a model of seismogenic sources for PSHA applications must include information on the 3rd dimension of faults. Constraints on the down-dip geometry of faults, on the thickness of the seismogenic layer as well as on the structural style at a regional scale allow us to define a more rigorous model of seismogenic sources. Compared to 2D seismogenic source models (surface trace of active faults, see Figure 1), 3D models are better constrained in both the geometry and the seismogenic potential of the faults. This approach has direct implications on PSHA. Differences between PSHA scenarios evaluated by using 2D or 3D source models are in the absolute value of the expected ground shaking as well as in its spatial distribution. For example, by using 3D seismogenic sources, the expected ground shaking is centred within the hanging wall of the sources; it is more realistic than that predicted by using 2D linear sources (compare Figure 1).

Open questions

Some questions still remain open: one concerns the segmentation model, e.g. the identification of boundaries between fault segments which will not be jumped by the largest expected earthquake; the second concerns the 'dialog' between adjacent sources at the time of an earthquake and the possibility of triggering of subsequent events on near faults (see Scholz and Gupta, 2000 for a discussion on these problems and related SHA implications).

Our segmentation model (Figure 3) is qualitative, being exclusively based on identification of first-order (kilometric scale) geometric or structural complexities. We consider such complexities as likely barriers between major earthquake segments. It is well known that structural–geometric observations alone cannot solve the problem unambiguously; but it can be a reasonable compromise until a more rigorous solution is found, possibly by implementation of observations on past earthquake history of faults (e.g. more paleoseismological data) and/or application of robust mechanical models (e.g. Scholz and Gupta, 2000 and references therein). Mechanical models should be able to consider also the role of pre-existing discontinuities in the interaction, linkage and possible barrier effects between pairs of normal faults. In fact, the presence of pre-existing discontinuities, locally reactivated as oblique-slip transfer faults and representing sharp bends along mechanically continuous fault system, is quite common in the Apennines of Italy (e.g. Pace et al., 2002a).

Concerning the second point (triggered events), a number of works have shown that variations in static stress produced by an earthquake, possibly aided by fluid migration, may trigger earthquakes on near faults

(Das and Scholz, 1981; King et al., 1994; Sibson, 2000). The earthquake history of central Apennines encompasses cases of triggered events as well as cases of large single events without triggering. Evident examples of compound events, likely induced by triggering effects, are the 1703 earthquakes on the Norcia, Montereale and Pizzoli–Mt. Pettino adjacent structures (January 14, 1703 I = XI M = 6.8 and February 2, 1703 I = X M = 6.7; Working Group CPTI, 1999 and references therein) as well as the recent 1997 earthquake sequence in the Colfiorito area (Amato et al., 1998; Cocco et al., 2000). An example of single large event without triggering is the M_s = 7.0 1915 earthquake on the Fucino fault (Ward and Valensise, 1989). Our geologic model cannot solve this problem but once the 3D geometry of faults, remote stress field and kinematics is known, stress variation induced by the expected earthquake on adjacent faults can be better evaluated and, possibly, a probability of occurrence of triggered events can be added to the PSHA scenarios.

Acknowledgments

The authors are grateful to R. Wahlstrom and F. Galadini for improving the manuscript with their critical reviews and suggestions. This study was supported by M.U.R.S.T. grants to G. Lavecchia.

References

Amato, A., Azzara, R., Chiarabba, C., Cimini, G.B., Cocco, M., Di Bona, M., Margheriti, L., Mazza, S., Mele, F., Selvaggi, G., Basili, A., Boschi, E., Courboulex, F., Deschamps, A., Gaffet, S., Bittarelli, G., Chiaraluce, L., Piccinini, D. and Ripepe, M., 1998, The 1997 Umbria-Marche, Italy, earthquake sequence; a first look at the main shocks and aftershocks, *Geophys. Res. Lett.* **25**, 2861–2864.

Barchi, M.R., De Feyter, A., Magnani, M.B., Minelli, G. Pialli, G. and Sotera, B.M., 1998, The structural style of the Umbria-Marche fold and thrust belt, *Mem. Soc. Geol. Ital.* **52**, 557–578.

Barchi, M., Galadini, F., Lavecchia, G., Messina, P., Michetti, A.M., Peruzza, L., Pizzi, A., Tondi, E. and Vittori, E. (eds.), 2000, *Sintesi Delle Conoscenze Sulle Faglie Attive in Italia Centrale: Parametrizzazione ai Fini Della Carattrizzazione Della Pericolosità Sismica*, Roma, CNR-Gruppo Nazionale per la Difesa dai Terremoti, 62 pp.

Basili, R., 1999, *La componente verticale della tettonica plio-quatrnaria in Appennino centrale.* PhD Thesis, Università degli Studi di Roma 'La Sapienza,' Roma (Italy), 108 pp.

Basili, R., Bosi, V., Galadini, F., Galli, P., Meghraoui, M., Messina, P., Moro, M. and Sposato, A., 1998, The Colfiorito earthquake sequence of September–October 1997: surface breaks and seismotectonic implications for the central Apennines (Italy), *J. Earthq. Eng*. **2**, 291–302.

Blumetti, A.M., 1995, Neotectonic investigations and evidence of paleoseismicity in the epicentral area of the January–February 1703, central Italy, earthquakes. In: L. Serva (ed.), *Perspectives in Paleoseismology*, Vol 6, pp. 83–100.

Boncio, P., 1998, *Analisi integrata di dati geologico-strutturali e sismologici per la definizione di un modello sismotettonico in Appennino umbro-marchigiano.* PhD Thesis, Università degli Studi di Perugia, Perugia (Italy), 107 pp.

Boncio, P., Brozzetti, F. and Lavecchia, G., 2000, Architecture and seismotectonics of a regional low-angle normal fault zone in central Italy, *Tectonics* **19**, 1038–1055.

Boncio, P. Brozzetti, F., Ponziani, F., Barchi, M., Lavecchia, G. and Pialli, G., 1998, Seismicity and extensional tectonics in the northern Umbria-Marche Apennines, *Mem. Soc. Geol. Ital.* **52**, 539–555.

Boncio, P. and Lavecchia, G., 2000a, A structural model for active extension in Central Italy, *J. Geodyn.* **29**, 233–244.

Boncio, P. and Lavecchia, G., 2000b, A geological model for the Colfiorito earthquakes (September–October 1997, Central Italy), *J. Seismol*. **4**, 345–356.

Boncio, P., Lavecchia, G., Milana, G. and Rozzi, B., 2004, Seismogenesis in Central Apennines, Italy: an integrated analysis of minor earthquake sequences and structural data in the Amatrice-Campotosto area, *Ann. Geophys.*, in press.

Bosi, C., 1975, Osservazioni preliminary su faglie probabilmente attive nell'Appennino centrale, *Boll. Soc. Geol. Ital.* **94**, 827–859.

Brozzetti, F. and Lavecchia, G., 1994, Seismicity and related extensional stress field: the case of the Norcia Seismic Zone (Central Italy), *Ann. Tectonicae* **8**, 36–57.

Byerlee, J.D., 1978, Friction of rocks, *Pure Appl. Geophys.* **116**, 615–626.

Calamita, F., Coltorti, M., Piccinini, D., Pierantoni, P.P., Pizzi, A., Ripepe, M., Scisciani, V. and Turco, E., 2000a, Quaternary faults and seismicity in the Umbro-Marchean Apennines (central Italy), *J. Geodyn.* **29**, 245–264.

Calamita, F. and Pizzi, A., 1994, Recent and active extensional tectonics in the southern umbromarchean Apennines (central Italy), *Mem. Soc. Geol. Ital.* **48**, 541–548.

Calamita, F., Pizzi, A., Scisciani, V., De Girolamo C., Coltorti, M., Pieruccini, P. and Turco, E., 2000b, Caratterizzazione delle faglie quaternarie nella dorsale appenninica umbro-marchigiana-abruzzese. In: F. Galadini, C. Meletti, and A. Rebez (eds.), *Le Ricerche del GNDT Nel Campo Della Pericolosità Sismica (1996–1999)*, CNR-Gruppo Nazionale per la Difesa dai Terremoti, Roma, 2000, pp. 157–169.

Cattaneo, M., Augliera, P., De Luca, G., Gorini, A., Govoni, A., Marcucci, S., Michelini, A., Monachesi, G., Spallarossa, D., Trojani, L. and XGUMS, 2000, The 1997 Umbria–Marche (Italy) earthquake sequence: analysis of the data recorded by the local and temporary networks, *J. Seismol.* **4**, 401–414.

Cavinato, G.P., Chiaretti, F., Cosentino, D. and Serva, L., 1989, Caratteri geologico-strutturali del margine orientale della conca di Rieti, *Bolle. Soc. Geol. Ital.* **108**, 207–218.

Cello, G., Deiana, G., Mangano, P., Mazzoli, S., Tondi, E., Ferreli, L., Maschio, L., Michetti, A. M., Serva, L. and Vittori, E., 1998, Evidence for surface faulting during the september 26, 1997, Colfiorito (Central Italy) earthquakes, *J. Earthq. Eng.* **2**, 303–324.

Cello, G., Mazzoli, S., Tondi, E. and Turco, E., 1997, Active tectonics in the central Apennines and possible implications for seismic hazard analysis in peninsular Italy, *Tectonophysics* **272**, 43–68.

Cinti, F.R., Cucci, L., Marra, F. and Montone, P., 2000, The 1997 Umbria-Marche earthquakes (Italy): relations between the surface tectonic breaks and the area of deformation, *J. Seismol.* **4**, 333–343.

Cocco, M., Nostro, C. and Ekstroem, G., 2000. Static stress changes and fault interaction during the 1997 Umbria-Marche earthquake sequence, *J. Seismol.* **4**, 501–516.

Collettini, C., Barchi, M., Pauselli, C., Federico, C. and Pialli, G., 2000, Seismic expression of active extensional faults in northern Umbria (central Italy), *J. Geodyn.* **29**, 309–321.

D'Agostino, N., Giuliani, R., Mattone, M. and Bonci, L., 2001, Active crustal extension in the central Apennines (Italy) inferred from GPS measurements in the interval 1994–1999, *Geophys. Res. Lett.* **28**, 2121–2124.

Das, S. and Scholz, C.H., 1981, Off-fault aftershock clusters caused by shear stress increase?, *Bull. Seism. Soc. Am.* **71**, 1669–1675.

De Luca, G., Scarpa, R., Filippi, L., Gorini, A., Marcucci, S., Marsan, P., Milana, G. and Zambonelli, E., 2000, A detailed analysis of two seismic sequences in Abruzzo, Central Apennines, Italy, *J. Seismol.* **4**, 1–21.

Deschamps, A., Iannaccone, G. and Scarpa, R., 1984, The Umbrian earthquake (Italy) of 19 September 1979, *Ann. Geophys.* **2**, 29–36.

Deschamps, A., Scarpa, R. and Selvaggi, G., 1989, Analisi sismologica del settore settentrionale dell'Appennino umbro-marchigiano, *Proceedings VIII Nat. Congr. G.N.G.T.S., Rome* **1**, 9–15.

Dragoni, M., Doglioni, C., Mongelli, F. and Zito, G., 1996, Evaluation of stress in two geodynamically different areas; stable foreland and extensional backarc, *Pure App. Geophys.* **146**, 319–341.

Ekstrom, G., Morelli, A., Boschi, E. and Dziewonski, A.M., 1998, Moment tensor analysis of the central Italy earthquake sequence of September–October 1997, *Geophys. Res. Lett.* **25**, 1971–1974.

Frankel, A., 1995, Mapping seismic hazard in the central and eastern United States, *Seismol Res. Lett.* **66**, 8–21.

Frepoli, A. and Amato, A., 1997, Contemporaneous extension and compression in the Northern Apennines from earthquake fault-plane solutions, *Geophys. J. Int.* **129**, 368–388.

Frepoli, A. and Amato, A., 2000, Spatial variations in stresses in peninsular Italy and Sicily from background seismicity, *Tectonophysics* **317**, 109–124.

Galadini, F. and Galli, P., 1999, The Holocene paleoearthquakes on the 1915 Avezzano earthquake faults (central Italy); implications for active tectonics in the central Apennines, *Tectonophysics* **308**, 143–170.

Galadini, F. and Galli, P., 2000, Active tectonics in the Central Apennines (Italy)—Input data for Seismic Hazard Assessment, *Nat. Hazards* **22**, 225–270.

Galadini, F. and Galli, P., 2001, Archaeoseismology in Italy: case studies and implications on long-term seismicity, *J. Earthq. Eng.* **5**, 35–68.

Galadini, F., Galli, P., Leschiutta, I., Monachesi, G. and Stucchi, M., 1999, Active tectonics and seismicity in the area of the 1997 earthquake sequence in central Italy: A short review, *J. Seismol.* **3**, 165–175.

Galadini, F., Meletti, C. and Vittori, E., 2000, Stato delle conoscenze sulle faglie attive in Italia: elementi geologici di superficie. In: F. Galadini, C. Meletti and A. Rebez (eds.), *Le Ricerche del GNDT Nel Campo della Pericolosità Sismica (1996–1999)*, CNR-Gruppo Nazionale per la Difesa dai Terremoti, Roma, 2000, pp. 107–136.

Galadini, F. and Messina, P., 2001, Plio-Quaternary changes of the normal fault architecture in the central Apennines (Italy), *Geodin. Acta* **14**, 321–344.

Gasperini, P., Bernardini, F., Valensise, G. and Boschi, E., 1999, Defining seismogenic sources from historical earthquake felt reports, *Bull. Seismol. Soc. Am.* **89**, 94–110.

Haessler, H., Gaulon, R., Rivera, L., Console, R., Frogneux, M., Gasparini, G., Martel, L., Patau, G., Siciliano, M. and Cisternas, A., 1988, The Perugia (Italy) earthquake of 29, April 1984: a microearthquake survey, *Bull. Seismol. Soc. Am.* **78**, 1948–1964.

King, G.C.P., Stein, R.S. and Lin, J., 1994. Static stress changes and the triggering of earthquakes, *Bull. Seismol. Soc. Am.* **84**, 935–953.

Kirby, S.H., 1983, Rheology of the Lithosphere, *Rev. Geophys. Space Phys.* **21**, 1458–1487.

Lavecchia, G., Boncio, P., Brozzetti, F., Stucchi, M. and Leschiutta, I., 2002, New criteria for seismotectonic zoning in Central Italy: insights from the Umbria-Marche Apennines, *Bolle. Soc. Geol. Ital.* **1**, 881–890.

Lavecchia, G., Brozzetti, F., Barchi, M., Keller, J. and Menichetti, M., 1994, Seismotectonic zoning in east-central Italy deduced from the analysis of the Neogene to present deformations and related stress fields, *Soc. Geol. Am. Bull.* **106**, 1107–1120.

Machette, M.N., 2000, Active, capable, and potentially active faults; a paleoseismic perspective, *J. Geodyn.* **29**, 387–392.

Mai, P.M. and Beroza, G.C., 2000, Source scaling properties from finite-fault-rupture models, *Bull. Seismol. Soc. Am.* **90**, 604–615.

Marsili, P. and Tozzi, M., 1991, Successione di eventi deformativi nei monti della Laga: il settore di Monte Gorzano (Rieti), *Studi Geol. Camerti* **1991/2**, 71–78.

Mc Calpin, J.P., 1996, *Paleoseismology*, Academic Press, San Diego, 588 pp.

Michetti, A.M., Brunamonte, F., Serva, L. and Vittori, E., 1996, Trench investigations of the 1915 Fucino earthquake fault scarps (Abruzzo, central Italy): geological evidence of large historical events, *J. Geophys. Res.* **101**, 5921–5936.

Michetti, A.M., Brunamonte, F., Serva, L. and Whitney, R.A., 1995, Seismic hazard assessment from paleoseismological evidence in the Rieti Region, Central Italy. In: L. Serva (ed.), *Perspectives in Paleoseismology*, Vol. 6, pp. 63–82.

Michetti, A.M. and Serva, L., 1990, New data on the seismotectonic potential of the Leonessa fault area (Rieti, central italy), *Rend. Soc. Geol. Ital.* **13**, 37–46.

Monachesi, G. and Stucchi, M. (eds.), 1997, DOM 4.1: un database di osservazioni macrosismiche di terremoti di area italiana al di sopra della soglia del danno (*an intensity database of damaging earthquakes in the Italian area)*, available on-line at *http://emidius.mi.ingv.it/DOM*.

Morewood N.C. and Roberts, G.P., 2000, The geometry, kinematics and rates of deformation within an en échelon normal fault segment boundary, central Italy, *J. Struct. Geol.* **22**, 1027–1047.

Pace, B., 2001, *Sorgenti sismogenetiche in Appennino centrale; definizione ed applicazione alle stime di pericolosità sismica.* PhD Thesis, Università degli Studi di Camerino-Chieti, Camerino (Italy), 144 pp.

Pace, B., Boncio, P. and Lavecchia, G., 2002a, The 1984 Abruzzo earthquake (Italy): an example of seismogenic process controlled by interaction between differently-oriented sinkinematic faults, *Tectonophysics* **350**, 237–254.

Pace, B., Peruzza, L., Lavecchia, G. and Boncio, P., 2002b, Seismogenic sources in Central Italy: from causes to effects, *Mem. Soc. Geol. Ital.* **57**, 419–429.

Pantosti, D., D'Addezio, G. and Cinti F.R., 1996, Paleoseismicity of the Ovindoli-Pezza fault, central Apennines, Italy: A history including a large, previously unrecorded earthquake in the Middle ages (860–1300 A.D.), *J. Geophys. Res.* **101**, 5937–5959.

Pasquale, V., Verdoya, M., Chiozzi, P. and Ranalli, G., 1997, Rheology and seismotectonic regime in the northern central Mediterranean, *Tectonophysics* **270**, 239–257.

Peruzza, L., (ed.), 1999, Progetto MISHA Metodi Innovativi per la Stima dell'HAzard: applicazione all'Italia Centrale, CNR-Gruppo Nazionale per la Difesa dai Terremoti, Roma, 176 pp.

Peruzza, L. and Pace, B., 2002, Sensitivity analysis for seismic source characteristics to probabilistic seismic hazard assessment in central Apennines (Abruzzo area), *Boll. Geofis. Teor. Appl.* **43**, 79–100.

Pizzi, A. and Scisciani, V., 2000, Methods for determining the Pleistocene-Holocene component of displacement on active faults reactivating pre-Quaternary structures: examples from the central Apennines (Italy), *J. Geodyn.* **29**, 445–457.

Ponziani, F., De Franco, R., Minelli, G., Biella, G., Federico, C. and Pialli, G., 1995, Crustal shortening and duplication of the Moho in the Northern Apennines; a view from seismic refraction data, *Tectonophysics* **252**, 391–418.

Ranalli, G. and Murphy, D.C., 1987, Rheological stratification of the lithosphere, *Tectonophysics* **132**, 281–295.

Rudnick, R.L. and Fountain, D.M., 1995, Nature and composition of the continental crust: a lower crustal perspective, *Rev. Geophys.* **33**, 267–309.

Scarascia, S., Lozej, A. and Cassinis, R., 1994, Crustal structures of the Ligurian, Tyrrhenian and Ionian seas and adjacent onshore areas interpreted from wide-angle seismic profiles, *Boll. Geofis. Teor. Appl.* **36**, 5–19.

Scholz, C.H., 1990, The mechanics of earthquakes and faulting, Cambridge University Press, Cambridge, 439 pp.

Scholz, C.H. and Gupta, A., 2000, Fault interactions and seismic hazard, *J. Geodyn.* **29**, 459–467.

Selvaggi, G., 1998, Spatial distribution of horizontal seismic strain in the Apennines from historical earthquakes, *Ann. Geofis.* **41**, 241–251.

Sibson, R.H., 1974, Frictional constraints on thrust, wrench and normal faults, *Nature* **249**, 542–544.

Sibson, R.H., 2000, Fluid involvement in normal faulting, *J. Geodynamics* **29**, 469–499.

Slejko, D., Peruzza, L. and Rebez, A., 1998, Seismic hazard maps of Italy, *Ann. Geofis.* **41**, 183–214.

Stirling, M.W., McVerry, G.H. and Berryman K.R., 2002, A new seismic hazard model for New Zealand, *Bull. Seismol. Soc. Am.* **92**, 1878–1903.

Stucchi, M., 1985, The earthquakes in central Italy, January–February 1703. Some questions, some preliminary answers, in D. Postpischl (ed.), *Atlas of Isoseismal Maps of Italian Earthquakes, Quaderni de La Ricerca Scientifica* **114**/2A, C.N.R., 56–57.

Valensise, G. and Pantosti, D. (eds.), 2001, Database of potential sources for earthquakes larger than M 5.5 in Italy, *Ann. Geofis.* **44**(Suppl.) 180 pp., with CD-ROM.

Vakov, A.V., 1996, Relationships between earthquake magnitude, source geometry and slip mechanism, *Tectonophysics* **261**, 97–113.

Vezzani, L. and Ghisetti, F., 1998, *Carta Geologica dell'Abruzzo* (1:100.000 scale), S.E.L.C.A., Firenze, 1998.

Walsh, J.J. and Watterson, J., 1988, Analysis of the relationship between displacements and dimensions of faults, *J. Struct. Geol.* **10**, 239–247.

Ward, S.N. and Valensise, G.R., 1989, Fault parameters and slip distribution of the 1915 Avezzano, Italy, earthquake derived from geodetic observations, *Bull. Seismol. Soc. Am.* **79**, 690–710.

Wells, D.L. and Coppersmith, K.J., 1994, New empirical relationships among magnitude, rupture length, rupture width, rupture area, and surface displacement, *Bull. Seismol. Soc. Am.* **84**, 974–1002.

WGCEP (Working Group on California Earthquake Probabilities), 1995, Seismic hazard in southern California: probable earthquakes, 1994 to 2024, *Bull. Seismol. Soc. Am.* **85**, 379–439.

Working Group CPTI, 1999, Catalogo Parametrico dei Terremoti Italiani, ING, GNDT, SGA, SSN (eds.), Bologna, 88 pp., available on-line at: http://emidius.mi.ingv.it/CPTI.